Temperature evolution of the crystal structures in $La(Mg_{1/2}Ti_{1/2})O_3$ perovskite: relation to the microwave dielectric properties

2008 J. Phys.: Condens. Matter 20 085210

(http://iopscience.iop.org/0953-8984/20/8/085210)

J. Phys.: Condens. Matter **20** (2008) 085210 (9pp) doi:10.1088/0953-8984/20/8/085210

Temperature evolution of the crystal structures in $La(Mg_{1/2}Ti_{1/2})O_3$ perovskite: relation to the microwave dielectric properties

Andrei N Salak[1], **Oleksandr Prokhnenko**[2] **and Victor M Ferreira**[3]

[1] Department of Ceramics and Glass Engineering/CICECO, University of Aveiro, 3810-193 Aveiro, Portugal
[2] Hahn-Meitner-Institut, Glienicker Straße 100, Berlin D-14109, Germany
[3] Department of Civil Engineering/CICECO, University of Aveiro, 3810-193 Aveiro, Portugal

E-mail: salak@cv.ua.pt, prokhnenko@hmi.de and victorf@ua.pt

Received 5 October 2007, in final form 9 January 2008
Published 1 February 2008
Online at stacks.iop.org/JPhysCM/20/085210

Abstract
The crystal structure and phase transition of the perovskite $La(Mg_{1/2}Ti_{1/2})O_3$ (LMT) have been investigated using high-resolution neutron powder diffraction in the temperature range 60–1414 K. Between 1246 and 1310 K LMT undergoes the monoclinic-to-rhombohedral ($P2_1/n$–$R\bar{3}$) crossover required by Landau theory to be a first order. The temperature dependences of the unit cell parameters and the octahedral tilt angles suggest a discontinuous phase transition. Specific variations of both the metal–oxygen bond lengths and the octahedra volume in LMT are correlated with the dielectric anomalies observed in the same temperature ranges. The uncommon dielectric behaviour in the vicinity of room temperature has been interpreted in terms of deformations of the TiO_6 octahedra which change their polarizability and thereby contribute to the dielectric response of LMT. It is believed that in spite of a generally negligible effect, such a contribution to the relative permittivity can occur in compositions containing oxygen octahedra as structural elements.

1. Introduction

Complex oxides with a perovskite structure are commonly considered as promising parent compositions for development of microwave resonators and filters. In order to optimize these materials for microwave applications, high values of both relative permittivity (ε_r) and quality factor (Q at the resonant frequency f_0) as well as a near-zero value of temperature coefficient of the resonant frequency (τ_f) should be achieved [1]. However, these fundamental parameters are inter-related and high-ε_r perovskites ordinarily demonstrate lossy and temperature dependent dielectric behaviour. Moreover, there is no rigorous criterion to predict dielectric properties of particular perovskite compounds and solid solutions in the gigahertz frequency range. As one of a few, the empirical relationship established by Reaney *et al* [2] expresses the crystal structure transformations involving an oxygen octahedral tilting in terms of the geometrical tolerance factor (t). Colla *et al* have shown [3], that such transformations govern both the magnitude of ε_r and its temperature variation. The temperature coefficient of permittivity (τ_ε) is related to τ_f as $\tau_f = -[\frac{1}{2}\tau_\varepsilon + \alpha_L]$, where α_L is the linear thermal expansion coefficient [3, 4]. Thus, both phase transitions and variations of thermal expansion can affect the fundamental microwave characteristics of perovskite dielectrics.

Lanthanum magnesium titanate, $La(Mg_{1/2}Ti_{1/2})O_3$ (LMT), was found to have ultra-high Q-factor (the highest value reported—16110 at $f_0 = 7.1$ GHz [5]) and a moderate relative permittivity. The value of ε_r reported by different authors varies between 27 and 33 (references [6] and [7], respectively). Similarly, the temperature coefficient of the resonant frequency was measured to be -65 and -100 ppm K^{-1} according to Cho *et al* [8] and Negas *et al* [7]. Whatever the case, the measured τ_f values are too far from a zero value. This drawback does not

allow using LMT itself in microwave devices. A doping or substitution with an adequate composition is required. In this way, the LMT-based perovskite solid solutions with promising microwave characteristics have been obtained [5, 6, 9, 10]. At the same time, the above-mentioned spread in values of the dielectric parameters has initiated more detailed investigations of lanthanum magnesium titanate. Our preliminary studies of dielectric response of LMT have revealed an uncommon temperature variation of both the relative permittivity measured at radio-frequency and the dielectric loss extrapolated from far infrared spectra in the vicinity of room temperature. The dielectric anomalies observed over a wide frequency range certainly suggest structure transition(s) which can affect the phonon spectrum of LMT.

In spite of a low value of the tolerance factor ($t = 0.945$), the crystal structure of LMT is not very distorted. Both the in-phase and anti-phase octahedral rotations (tilts) effectively compensate atomic size mismatch and, as a result, XRD reflections of LMT are only slightly split. This is why the crystal structure symmetry of LMT was a matter of discussion for a long time. The structure of lanthanum magnesium titanate was refined as cubic $Pa3$ [11], orthorhombic $Pnma$ [12] and finally monoclinic $P2_1/n$ [13]. At the present time it is accepted that at room temperature LMT has the monoclinic symmetry with the rocksalt-type ordering between Mg^{2+} and Ti^{4+} cations and the $a^-b^+a^-$ octahedral tilting (in Glazer's notation [14]) [15, 16]. A recent transmission electron microscopy study has not disproved the monoclinic $P2_1/n$ symmetry of LMT [17]. At the same time, indications of the high strain fields were revealed in this compound at room temperature [17]. Unfortunately, a laboratory XRD is not sensitive enough to judge the actual oxygen sublattice configuration and its variation with temperature. It should also be noted that no high-resolution diffraction study has been performed so far on this perovskite composition at any temperature.

It is known that increasing temperature or increasing the tolerance factor t generally results in the same effect. Thus, the data on structure instability and/or phase transitions in LMT (namely, their origin and the temperature ranges where these phenomena occur) are not only of fundamental interest. Based on these data, compositional variation of crystal structure and thereby dielectric properties of many LMT-based solid solutions can be predicted.

In this work, high-resolution neutron diffraction experiments on the perovskite LMT at particular temperature ranges have been performed. The obtained data are analysed in respect of the oxygen octahedral tilts and distortions and discussed in relation to the dielectric anomalies observed within the same temperature ranges.

2. Experimental details

Ceramic samples of LMT were prepared using the powders obtained by a chemical route [18] based on the Pechini method. This non-conventional route has been shown to allow producing nano-size powders as the starting material for fine-grain, homogeneous ceramics [5, 6]. In order to achieve the highest density, pellets of 20 mm in diameter and about 2 mm thick were uniaxially pressed into discs, placed on a platinum foil, and sintered in air at 1870 K. The sintering time was 4 h, heating and cooling rates did not exceed 10 K min^{-1}. For dielectric measurements, cylindrical samples of 10 mm in diameter and 8–10 mm length were isostatically pressed at 200 MPa and sintered under the same conditions.

The samples destined for diffraction experiments were ground with mortar and pestle. XRD characterization of phase content and crystal structure of sintered LMT were performed with Rigaku D/MAX-B diffractometer (Cu Kα radiation, tube power 40 kV, 30 mA, graphite monochromator, receiving slit of 0.15 mm, angular range $10° < 2\theta < 120°$, step of 0.02°, and exposition of 10 s/step) at room temperature. Neutron diffraction patterns were recorded using the fine-resolution powder diffractometer (FIREPOD-E9) with incident neutrons of wavelength $\lambda = 1.797$ Å at the Berlin Neutron Scattering Center (BENSC). Data were collected over the angular range $0° < 2\theta < 160°$. Low-temperature experiments (60–290 K) were performed in an Orange Standard helium cryostat (OS). A high temperature furnace (HTF) was used between 295 and 1420 K. The obtained data were refined by the Rietveld method using the FULLPROF suite [19].

The samples for radio-frequency dielectric investigations were polished to form disks of about 0.5 mm thick, electroded with platinum paste, and annealed at 1270 K for 2 h. Dielectric permittivity and loss tangent were measured as a function of temperature within a frequency range 10^2–10^6 Hz using a Precision *LCR* metre (HP 4284A). The measurements were performed on both heating and cooling with a rate of 1.5 K min^{-1} using an environment chamber (Delta Design 9023, 95–480 K) and a furnace (300–650 K). The room-temperature permittivity, Q-factor and resonant frequency of the cylindrical samples were estimated by an adaptation of the Hakki–Coleman method [20, 21] using a 10 MHz–20 GHz Scalar Analyzer (IFR 6823). The τ_f values were evaluated by measuring a temperature variation of the resonant frequency on cooling between 230 and 300 K with a rate of 2 K min^{-1}. The measurements were carried out in an oxygen-free cavity of high-conductivity copper, cooled by a CTI Cryogenics Model 22 refrigerator.

3. Results and discussion

3.1. Crystal structure

It was verified by XRD that single-phase perovskite LMT is obtained under the above-mentioned sintering conditions. The monoclinic perovskite structure was identified by visual inspection and comparison with the room-temperature diffraction patterns of LMT reported by Avdeev *et al* [15]. Indeed, using the collected XRD data, the monoclinic crystal structure ($P2_1/n$ space group) was successfully refined with the unit cell parameters $a = 5.5640(2)$ Å, $b = 5.5765(2)$ Å, $c = 7.8667(3)$ Å, $\beta = 90.044(8)°$. These parameters have been found to be in excellent agreement with those most recently ascribed to perovskite LMT by Vanderah *et al* [16].

The temperature range of interest was designated from the anomalous-like behaviour of the dielectric response of

LMT in the vicinity of room temperature. Another range was chosen to cover an expected interval of the first-order phase transition estimated from compositional variation of both structure and dielectric parameters in LMT-based perovskite solid solutions [22, 23]. Therefore, detailed (by short temperature steps) neutron diffraction experiments were performed between 170 and 330 K as well as over 1246–1414 K. Supplementary temperature points (60, 700 and 900 K) were also involved in the data collection in order to complete the picture of the temperature evolution of the structure parameters.

Representative parts of the neutron diffraction patterns of LMT at particular temperatures are shown in figure 1. The superlattice reflections arising from *B*-site cation ordering (1/2 1/2 1/2), antiparallel displacements of *A*-site cations—1/2{*even*, *even*, *odd*}, in-phase octahedral tilting— 1/2{*odd*, *odd*, *even*}, and anti-phase tilting— 1/2{*odd*, *odd*, *odd*} ($h + k + l > 3$) are clearly seen testifying to the monoclinic $P2_1/n$ symmetry of LMT at lower temperatures. (Hereafter, the indexing is presented in the primitive perovskite unit cell.) It should be noted that these reflections are generally more intense than those observed in the respective XRD patterns. Increasing temperature results in degeneration of the superlattice reflections associated with *A*-cation displacement and in-phase tilting ((1 1/2 0)/(3/2 1 0) and (3/2 1/2 0)/(3/2 1/21) in figure 1, respectively). These reflections were revealed to decrease gradually above room temperature and vanish between 1246 and 1310 K. At the same time, no visible variation of the intensities of other superlattice peaks has been observed. This suggests that only in-phase rotations of the oxygen octahedra disappear in this temperature range. Hence, possible anti-phase tilted systems proposed by a group-theoretical analysis for the B-cation 1:1 ordered (double) perovskites [24] were then considered. Taking into account that increasing temperature does not lower the crystal symmetry, $a^-b^0a^-$ (monoclinic $I2/m$), $a^0a^0c^-$ (tetragonal $I4/m$), and $a^-a^-a^-$ (rhombohedral $R\bar{3}$) are the only candidates. Therefore, the diffraction patterns of LMT within 60–1246 K were refined with the monoclinic $P2_1/n$ space group; the three anti-phase tilted systems were attempted for the data collected at 1310 K and above. Direct temperature transition between the monoclinic $P2_1/n$ and the tetragonal $I4/m$ phases has been observed in Sr-based tungstate perovskites [25, 26]. However, the case of $P2_1/n$–$I4/m$ crossover in LMT was eliminated at the initial stage of the analysis. Inspection of the diffraction pattern recorded at 1310 K has revealed that the profiles of the most indicative fundamental reflections, such as (*hhh*) and (*h*00), could not be described adequately using a tetragonal metric of the primitive perovskite unit cell. Indeed, a refinement with $I4/m$ space group has not yielded any acceptable result.

One could expect that the likely temperature-induced transition observed in LMT is a transformation from the $a^-b^+a^-$ tilt configuration to $a^-b^0a^-$. A continuous transition $P2_1/n$–$I2/m$ has recently been reported for some barium double perovskites [27, 28]. At the same time, a first-order crossover to the rhombohedral $R\bar{3}$ phase is also allowed [24]. It was possible to refine the diffraction data on LMT at

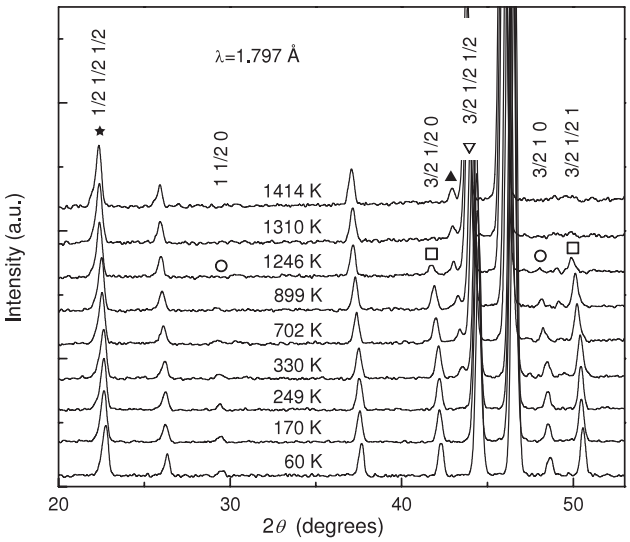

Figure 1. Neutron diffraction patterns of LMT recorded over the temperature range 60–1414 K. The peaks with fractional indexing are the superstructure reflections indicating Mg/Ti ordering (⋆), antiparallel La displacement (○), in-phase octahedral tilting (□), and anti-phase octahedral tilting (▽). The peak near 43° (▲) is reflection from the heating element of HTF, and has been excluded from the refinement.

1310 K with either $I2/m$ or $R\bar{3}$ space group. The latter provided a better fit in respect of both the description of the diffraction profiles and the values of the reliability factors: $I2/m$: $R_p = 4.47\%$, $R_{wp} = 5.75\%$, $\chi^2 = 2.11$; $R\bar{3}$: $R_p = 3.99\%$, $R_{wp} = 5.06\%$, $\chi^2 = 1.62$. Thus, the high-resolution diffraction patterns recorded below 1246 K and above 1310 K have successfully been refined using the monoclinic $P2_1/n$ space group (tilt system $a^-b^+a^-$) and the rhombohedral $R\bar{3}$ ($a^-a^-a^-$), respectively (figure 2). Typical values of the structure parameters of LMT at the lowest and highest available temperatures are listed in table 1. The refinement has also revealed that the Mg/Ti ordering rate remains essentially unchanged (∼94%) over the whole temperature range under study. The order-disorder ($Fm\bar{3}m$–$Pm\bar{3}m$) transition temperature for LMT was estimated by Levin *et al* [22] to be about 1900 K—well above the highest temperature applied in our study.

3.2. Phase transition and tilting/distortion of the oxygen octahedra

Based on the refined structure data and the unit cell relations reported in [10], the parameters of the primitive perovskite unit cell of LMT have been calculated. Their temperature variation is shown in figure 3. The $P2_1/n$–$R\bar{3}$ phase transition is required by Landau theory to be a first-order [24]. Indeed, a discontinuity in the temperature dependence of the unit cell parameters is observed in the vicinity of the crossover. The temperature variation of the primitive perovskite unit cell volume (V_p) has also been found to testify to a discontinuous character of the transition. Figure 4 represents the average parameter of the unit cell ($\bar{a}_p = V_p^{1/3}$) as a function of

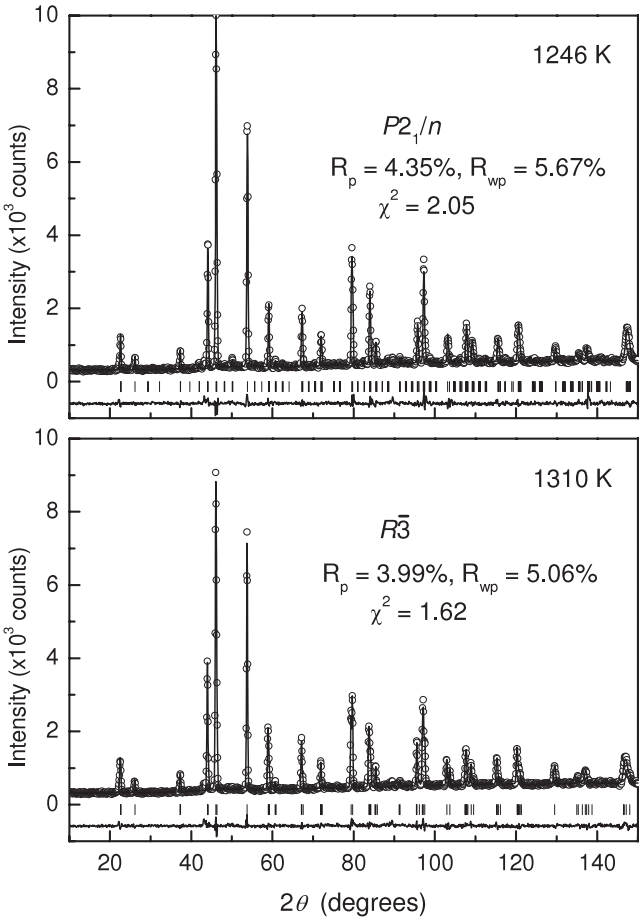

Figure 2. Observed (○), calculated (solid line), and difference (below) patterns of the neutron diffraction data along with the calculated peak positions (vertical bars) at 1246 K (refined in space group $P2_1/n$, top panel) and 1310 K ($R\bar{3}$, bottom panel).

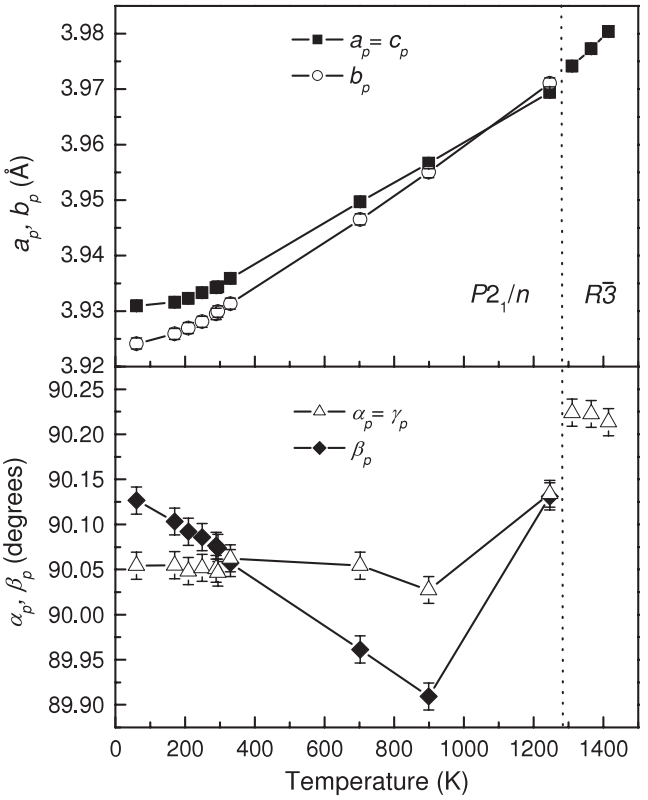

Figure 3. Primitive perovskite unit cell parameters (a_p, b_p, c_p and α_p, β_p, γ_p) of LMT as a function of temperature. The solid lines are guides to the eye.

temperature. As seen, the $\bar{a}_p(T)$ plot changes its slope between 1246 and 1310 K indicating a jump in the value of the linear thermal expansion coefficient (10.0 and 15.9 ppm K^{-1} below and above the transition, respectively).

The temperature variation of the unit cell parameters is not straightforward even within the range of the same (monoclinic $P2_1/n$) crystal symmetry of LMT (figure 3). It concerns mainly the unit cell angles; in particular, β_p. Between 900 and 1246 K a_p becomes less than b_p; at the same time, in this temperature range these parameters are very close in magnitude. As a result, the crystal structure of LMT at 1246 K looks similar to rhombohedral. Nevertheless, an attempt to refine the model $P2_1/n + R\bar{3}$ has yielded a negligible amount of the rhombohedral phase in LMT at this temperature. The anomalous-like state of LMT at 1246 K seems to be a result of some pre-organization effect(s) when approaching the first-order phase transition. Unfortunately, no diffraction data within the range 900–1246 K were collected and thus we cannot conclude unambiguously on a nature of this state.

In general, a drastic variation of the unit cell parameters does not always reflect actual phase transition. A similar phenomenon was observed for both compositional and temperature variations of cell parameters in several perovskite systems [10, 26, 27]. Zhou *et al* [26] attributed this to a change in the lattice strain not associated with structure phase transition. It should be noted that the non-monotonic variation of the unit cell angles of LMT occurs at the same temperature range (in the vicinity of 1000 K) where the metric of the primitive perovskite unit cell looks a near-cubic ($a_p = c_p = b_p$, $\alpha_p = \gamma_p \approx \beta_p \approx 90°$). Whatever the case, this phenomenon certainly needs a detailed analysis.

Slowing down of the temperature variation of the unit cell parameters (a_p, b_p and $\bar{a}_p$) observed below about 300 K (figures 3 and 4) is due to the quantum effect resulting in the saturation of thermal expansion of solids at low temperatures [29]. Such saturation behaviour of temperature dependence of a lattice parameter can be described by [29]:

$$a = a_0 + a_1\theta_S \coth\left(\frac{\theta_S}{T}\right). \quad (1)$$

The $\bar{a}_p(T)$ dependence for the temperature range of the monoclinic phase has been found to follow well equation (1) with the saturation temperature $\theta_S \sim 250$ K (figure 4).

The angles of the in-phase (ψ) and anti-phase (ϕ) oxygen octahedra rotations in LMT were calculated from the refined atomic coordinates using the formulae given in [28]. In a double perovskite, $A(B'_{1/2}B''_{1/2})O_3$, the tilt angles of the $B'O_6$ and $B''O_6$ octahedra are related in the inverse ratio of the B′–O and B″–O bond lengths [28]. Thus the change in tilt angles is governed by change in the respective bond

Table 1. Representative structure parameters for two distinct phases of $La(Mg_{1/2}Ti_{1/2})O_3$ obtained from Rietveld refinement of the neutron diffraction data.

Atom	Site	x	y	z	B_{iso} (Å^2)	Occupation
La	4*e*	0.4959(23)	0.5313(5)	0.2508(14)	0.22(4)	1
Mg1	2*d*	0.5	0	0	0.15(10)	0.942(3)
Ti1	2*d*	0.5	0	0	0.15(10)	0.058(3)
Ti2	2*c*	0	0.5	0	0.07(12)	0.942(3)
Mg2	2*c*	0	0.5	0	0.07(12)	0.058(3)
O1	4*e*	0.2723(14)	0.2895(16)	0.0371(13)	0.32(15)	1
O2	4*e*	0.2062(12)	0.7768(16)	0.0418(12)	0.09(13)	1
O3	4*e*	0.5773(11)	0.9855(9)	0.2532(12)	0.49(9)	1
	B_{11} (Å^2)	B_{22} (Å^2)	B_{33} (Å^2)	B_{12} (Å^2)	B_{13} (Å^2)	B_{23} (Å^2)
La	0.005(2)	0.0003(1)	0.0003(5)	−0.002(2)	0.0037(15)	0.0006(1)
O1	0.002(3)	0.0028(28)	0.0015(17)	0.0096(24)	−0.0011(18)	−0.0025(19)
O2	−0.0046(26)[a]	0.0054(34)	−0.0015(16)[a]	0.0067(23)	−0.0030(15)	−0.0009(2)
O3	0.0005(2)	0.0112(25)	0.0001(1)	−0.002(1)	0.0029(22)	0.0025(25)
$T = 60$ K, space group $P2_1/n$, cell parameters: $a = 5.5531(3)$ Å, $b = 5.5654(3)$ Å, $c = 7.8483(4)$ Å, $\beta = 90.077(7)°$, reliability factors: $R_p = 4.52\%$, $R_{wp} = 6.14\%$, $\chi^2 = 1.83$						
La	6*c*	0	0	0.2510(3)	2.37(5)	1
Mg1	3*a*	0	0	0	1.52(12)	0.948(2)
Ti1	3*a*	0	0	0	1.52(12)	0.052(2)
Ti2	3*b*	0	0	0.5	1.25(19)	0.948(2)
Mg2	3*b*	0	0	0.5	1.25(19)	0.052(2)
O	18*f*	0.3210(9)	0.1044(5)	0.4181(3)	3.31(7)	1
	B_{11} (Å^2)	B_{22} (Å^2)	B_{33} (Å^2)	B_{12} (Å^2)	B_{13} (Å^2)	B_{23} (Å^2)
La	0.0188(5)	0.0188(5)	0.0031(2)	0	0	0
O	0.0273(13)	0.0383(17)	0.0048(1)	0.0158(15)	0.0056(3)	0.0033(6)
$T = 1414$ K, space group $R\bar{3}$, cell parameters: $a = 5.6396(2)$ Å, $c = 13.7371(5)$ Å, reliability factors: $R_p = 3.78\%$, $R_{wp} = 4.94\%$, $\chi^2 = 1.56$						

[a] The obtained negative values of B_{11} and B_{33} are not statistically significant.

lengths. The difference between the tilt angles of the MgO_6 and TiO_6 octahedra in LMT was found to be mainly minor and regular, although small variations of $\psi(MgO_6)$ and $\psi(TiO_6)$ in opposite way were detected in some temperature ranges. In order to clarify the general temperature trend of the tilt angles, their average values were considered. Details on the specific behaviour of the Mg–O and Ti–O bond lengths will be given below.

It is known that the octahedral tilt angle can be regarded as the order parameter (Q) [30]. The temperature variation of Q in the vicinity of a continuous phase transition ($T \leqslant T_C$, T_C—the transition temperature) is ordinarily given by

$$Q^2 \propto 1 - \frac{T}{T_C}. \tag{2}$$

Another form of the $Q(T)$ dependence allows for a low-temperature saturation effect [29, 31]:

$$Q^2 \propto 1 - \frac{1}{T_C}\left(\theta_S \coth\left(\frac{\theta_S}{T}\right)\right). \tag{3}$$

Equation (3) transforms to equation (2) when $T \gg \theta_S$. A continuous phase transition involving the oxygen octahedra tilting can be either a second-order (tilt angle is the order parameter) or a tricritical in nature (square angle is the order parameter) [30].

The average values of the tilt angles versus temperature are represented in figure 4. The expected phase transition from the rhombohedral $R\bar{3}$ to the cubic $Fm\bar{3}m$ phase in LMT [22] is associated with a continuous disappearance of the anti-phase octahedral tilting [24]. T_C of this transition (∼1750 K) has been estimated from the compositional behaviour of crystal structure in the LMT-based solid solutions [22]. Since the data were only available for the anti-phase tilt angle at lower temperatures, including the range where quantum saturation is expected, we fitted $\phi(T)$ with equation (3), $\phi \equiv Q$ (figure 4). It has been shown above that the phase transition revealed in the range of 1246–1310 K (monoclinic, $\psi \neq 0$—rhombohedral, $\psi = 0$) appears to be a first-order. Nevertheless, the observed temperature variation of the in-phase tilt angle in LMT was also fitted using both ψ and ψ^2 as Q. It is seen from figure 4, a discontinuous character of the $P2_1/n$–$R\bar{3}$ structure transformation is evidently confirmed by the temperature variation of $\psi(T)$ in the vicinity of the crossover. The in-phase tilt angle gets abruptly a zero value that is typical of a first-order phase transition.

Magnitude of the anti-phase tilt angle in LMT in the saturation range (see figure 4) is very close to that reported for the B-site ordered perovskite $BaBiO_3$ ($Ba_2Bi^{3+}Bi^{5+}O_6$): $\phi \sim 12°$ estimated in the region of its monoclinic phase $P2_1/n$ at 4.2 K [28]. Regarding the in-phase tilt angle, it is about

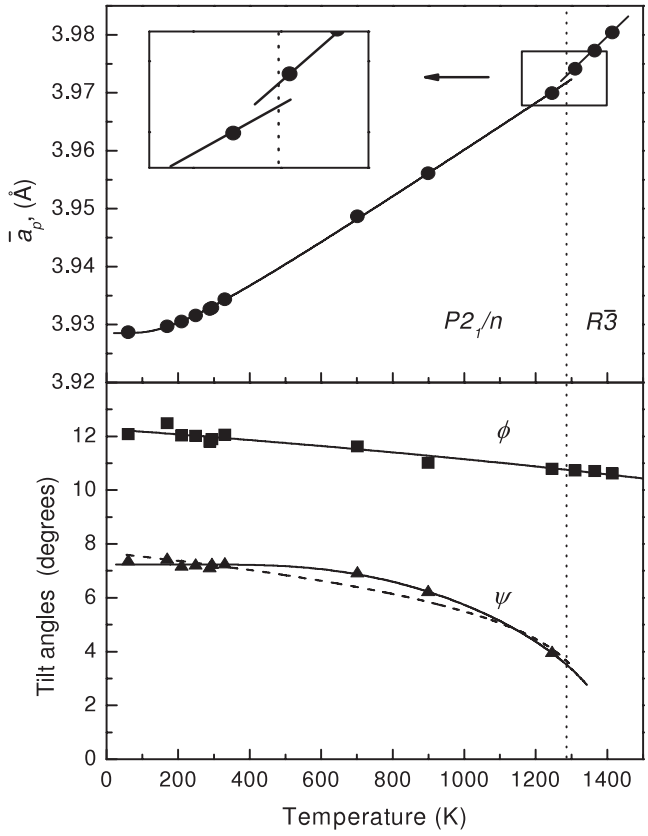

Figure 4. Temperature dependence of the average parameter of the primitive perovskite unit cell ($\bar{a}_p = V_p^{1/3}$, top) fitted with equation (1) (solid line). Temperature variations of the in-phase (ψ) and anti-phase (ϕ) tilt angles (bottom) fitted with equation (3)—ψ and ϕ as the order parameters (solid lines), and equation (2)—ψ^2 as the order parameter (dashed line).

7° for LMT versus $\psi \sim 3.5°$ for $BaBiO_3$. One should note, however, that in-phase tilting in the latter disappears at much lower temperature ($T_C \approx 140$ K). When the anti-phase tilt axis switches discontinuously from $[110]_p$ to $[111]_p$ at the $P2_1/n$–$R\bar{3}$ crossover in LMT, only a little change in the ϕ value takes place (figure 4). It is similar to that reported for $BaBiO_3$, although such switching in the latter occurs through the $I2/m$–$R\bar{3}$ transition [28].

The obtained results confirm that LMT undergoes the first-order phase transition from the monoclinic $P2_1/n$ to the rhombohedral $R\bar{3}$ structure without an intermediate phase. Many of double perovskites with a relatively small A-site cation adopt the monoclinic $P2_1/n$ structure [24, 32], since the respective $a^-b^+a^-$ tilt configuration is often the most stable at low temperatures [33]. Different sequences of the structure transformations from the monoclinic $P2_1/n$ to the highest symmetry cubic $Fm\bar{3}m$ phase were revealed in such perovskites. The series $P2_1/n$–$I2/m$–$R\bar{3}$–$Fm\bar{3}m$ [28] and $P2_1/n$–$I4/m$–$Fm\bar{3}m$ [25, 26] seem the most natural and complete [24]. Nevertheless, other series of the transitions are also known; specifically, that *via* $C2/c$ ($a^0b^+c^-$) and $P4/mcm$ ($a^0a^0c^+$) [34]. In some cases the structure transformations occur without either the intermediate $R\bar{3}$ [27] or $I2/m$ phase (as with LMT). Direct $P2_1/n$–$Fm\bar{3}m$ crossover has also been reported [35]. As mentioned in Introduction, the phase transitions involving the oxygen octahedra rotations generally exert influence on the fundamental dielectric parameters of perovskite systems. A number of such systems have already been studied in respect of the structure transitions; nevertheless, a generalization of their possible sequences in terms of the properties of the particular atoms involved (size, oxidation state etc) has not been performed yet. It is certainly a matter of the systematic investigation.

Along with the tilt angles, the temperature variations of the bond lengths in LMT were also evaluated. As known, the coordination number (CN) of the A-site cation in the ideal perovskite structure is 12. In non-cubic perovskites, the respective structure distortions result in a smaller CN [33]. It has been found that CN of La in LMT is changed in the temperature interval close to room temperature. In particular, when $T \leqslant 210$ K the first coordination sphere around lanthanum includes eight oxygen anions. The coordination number is eight again at 250 K, while for $T \geqslant 290$ K it is invariably nine regardless of the $P2_1/n$–$R\bar{3}$ crossover. Owing to the distorted structure of LMT, it was difficult to elucidate the temperature behaviour of each of the twelve La–O distances. At the same time, we found that the temperature variation of the average value of the La–O bond lengths is very similar to the $\bar{a}_p(T)$ dependence (see figure 4). Correspondingly, the bond valence sum (BVS) of lanthanum demonstrates a general trend to decrease with temperature. Nevertheless, some scatter of the BVS values in the vicinity of room temperature and a small jump associated with the first-order phase transition are also observed. BVS of La in LMT at 295 K is 2.77(5), slightly farther from the ideal valence than that reported for the isostructural perovskite $La(Zn_{1/2}Ti_{1/2})O_3$ (LZT) which presents 2.928 at room temperature [36].

The oxygen octahedra are known to constitute the framework of the perovskite structure. As a result, in an individual BO_6 octahedron, differences between the B–O bond lengths and their temperature variations are incomparably smaller than the observed for the A–O distances [28]. Indeed, the average B–O bond lengths in LMT have been revealed to be essentially temperature independent: 2.066(8) Å and 1.955(3) Å for Mg–O and Ti–O, respectively (cf 2.0909 Å and 1.9545 Å for Zn–O and Ti–O in LZT [36]). The corresponding BVS for Mg/Ti are 2.19(4)/4.12(5) over the whole temperature range investigated. At the same time, the ranges of a specific behaviour of the metal–oxygen distances in the MgO_6 and TiO_6 octahedra are observed around both room temperature and the phase transition. Figure 5 shows the temperature variations of the Ti–O bond lengths in LMT. It should be noted that the changes in the respective Mg–O and Ti–O distances occur in the anti-phase manner. It was also estimated that in the vicinity of room temperature the volume of the TiO_6 octahedra varies within 0.9%, whereas it jumps by 1.7% at the discontinuous $P2_1/n$–$R\bar{3}$ phase transition (figure 5). For the MgO_6 octahedra (not shown) these variations are 1.0 and 0.6%, respectively. At the same time, the difference between the values of the TiO_6 octahedra volume at the lowest and the highest temperatures applied (60 and 1414 K) is only ∼0.1%.

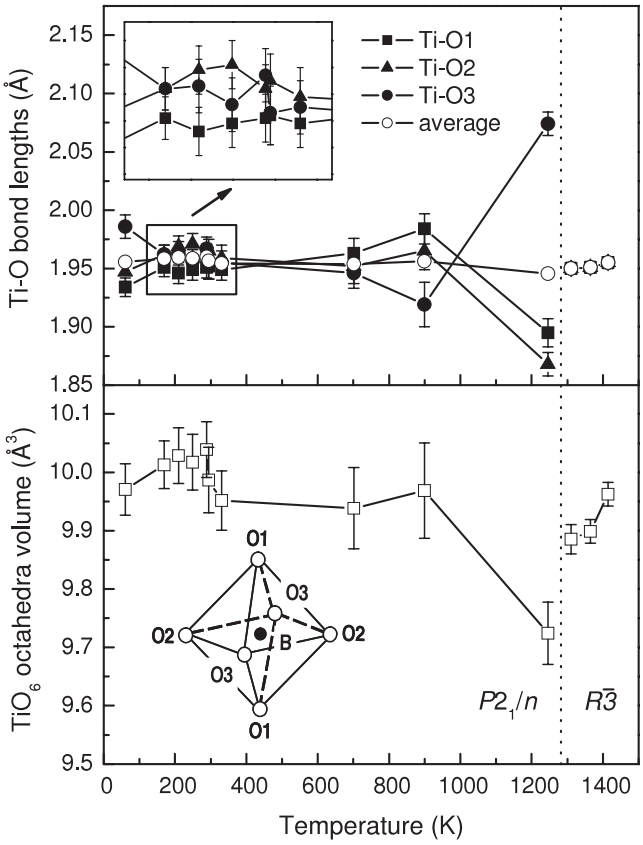

Figure 5. The Ti–O bond lengths and the TiO_6 octahedra volume in LMT as a function of temperature.

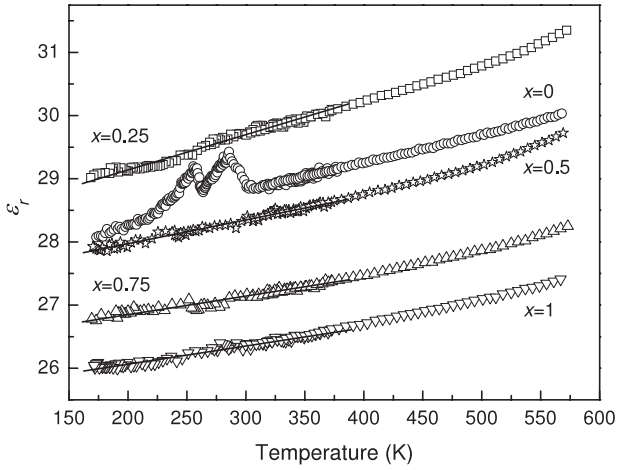

Figure 6. Temperature dependence of relative permittivity (ε_r) measured at 1 MHz for the $(1-x)$LMT–xNMT ceramics. (Open symbols and solid lines represent experimental data and linear fit, respectively. The gradual deviation from the linear dependence observed in some mixed compositions with increasing temperature above ∼400 K is attributed to the thermo-activated hopping conduction of localized charges).

3.3. Dielectric behaviour

The relatively high permittivity of non-ferroelectric perovskites is commonly associated with cations of the transition metals of IV–VI groups (such as Ti^{4+}, Nb^{5+}, W^{6+}) inside the oxygen octahedra [37–39]. Due to their specific electronic configuration and the chemical bound involving these cations, the respective metal–oxygen octahedra possess the essential polarizability and in applied fields they behave as the linked polar entities [40]. In LMT the TiO_6 octahedra are certainly such polar units.

It has experimentally been proved that the oxygen octahedra rotations in perovskites affect both the dielectric permittivity and its temperature variation [2, 3]. In its turn, it alters the value of their temperature coefficient of the resonant frequency [41]. Hence the first-order phase transition ($P2_1/n$–$R\bar{3}$) in LMT is also expected to result in a change of τ_f, although a direct confirmation based on dielectric measurements is hardly possible because of too high T_C. As observed, this phase transition is associated with the distinctive variations of the B–O distances and the BO_6 octahedra volume (figure 5). It is also seen that these parameters demonstrate specific temperature behaviour between about 170 and 300 K. A character of deformation of the octahedra changes within this temperature interval: the longer Ti–O bond length gets the shortest and vice versa. Moreover, this is the range where the TiO_6 octahedra volume reaches the maximal value.

Radio-frequency dielectric measurements on LMT were performed along with the ceramics of the $La_xNd_{1-x}(Mg_{1/2}Ti_{1/2})O_3$ system [42]. Neodymium magnesium titanate (NMT) and LMT are isostructural perovskites [43] and the crystal structure of their solid solutions is entirely described using the same $P2_1/n$ space group. Figure 6 shows the relative permittivity of the $(1-x)$LMT–xNMT ceramics measured as a function of temperature at 1 MHz. No substantial anomalies are detected over the presented temperature interval for all the compositions under study, except for that with $x = 0$ (pure LMT). For this composition the deviation of $\varepsilon_r(T)$ from the linearity is ∼2.5% (at about 285 K). It should be pointed that the anomaly is observed at the temperature range where no real phase transition occurs. In spite of the essential structure similarity of the end members, the compositional variations of both ε_r and τ_f for LMT–NMT are non-linear and even non-monotonic (figure 7). Since no structural transition has been observed for all the compositions of the system (at least, within the temperature range where these dielectric parameters were estimated), one could expect a near-linear dependence of τ_f on ε_r [4, 41]. This has actually been found to be the case for most of the compositions; nevertheless, the point associated with LMT evidently falls out from the trend (figure 8). All these facts suggest again a particular dielectric behaviour of LMT in the vicinity of room temperature.

Let us suppose that a distortion of the metal–oxygen octahedra results in a variation of the dielectric response of the respective solid (in particular, perovskite composition) just as a structural phase transition (including the transition which involves the octahedral tilting) does. It has been shown that the main contribution to the dielectric permittivity of the cubic double perovskites comes from the first two of their four polar-phonon modes, namely those corresponding to $A \leftrightarrow BO_6$ vibrations and $B \leftrightarrow O_6$ stretching [38]. Competition between temperature variations of the strongest modes determines the

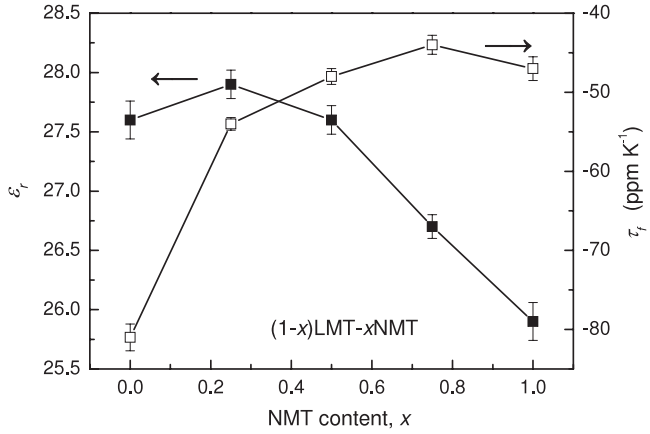

Figure 7. Compositional dependence of relative permittivity (ε_r, solid symbols) and temperature coefficient of the resonant frequency (τ_f, open symbols) measured at a gigahertz frequency range for the $(1-x)$LMT–xNMT system [42].

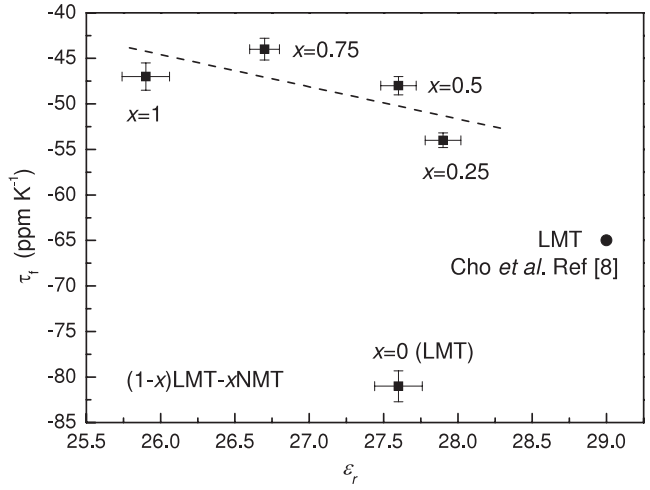

Figure 8. τ_f versus ε_r for the $(1-x)$LMT–xNMT ceramics.

behaviour of $\varepsilon_r(T)$ [44]. Distorted perovskites (e.g. LMT) have more complicated polar-phonon spectra [6]; nevertheless, the principal contributors to their permittivity are of the same origin. We believe that deformations of the BO_6 octahedra in respect of both shape and volume can modify the vibration mode(s) and thereby affect the dielectric response. The polar units of LMT—the TiO_6 octahedra are notably distorted at room temperature. A degree of their distortion (the relative ratio of the longest and shortest Ti–O distances) is 1.12% in comparison with 0.34% for the isostructural perovskite LZT [36]. Moreover, as mentioned above, a character of deformation of the octahedra in LMT alters between about 170–300 K (figure 5). As a result, direction and/or available space for displacements of Ti^{4+} in the octahedra and hence the polarizability of these polar units are changed.

Irregular twin domains and dislocations indicative of the high strain fields have recently been revealed in LMT at standard conditions [17]. One can suppose that in the vicinity of room temperature the crystal lattice of this composition is at the stage of some internal relaxation-like process. Local strain seems to be partially released by means of re-distribution of bond distances resulting in certain modification(s) of the coordination geometry. (Recall the observed change in CN of lanthanum in LMT.) At the same time, a relatively low symmetry of the LMT crystal structure can allow some re-arrangement of the atoms within the same space group $P2_1/n$. We also guess that the particular pattern of the lattice strain in LMT and ways of the strain release are very individual and sensitive to its composition and microstructure. It would explain the spread in the data on the microwave dielectric characteristics of LMT reported by different authors [5, 7, 8] (see also figure 8). On the other hand, it is believed that the suggested effect of distortion of the metal–oxygen octahedra on the dielectric behaviour has universal character. However, the contribution to ε_r due to such a phenomenon is rather negligible and can be detected (if any) only in the compositions with a moderate permittivity.

4. Conclusions

The high-resolution neutron diffraction data on LMT have been refined using the monoclinic $P2_1/n$ space group (tilt system $a^-b^+a^-$) below 1246 K and the rhombohedral $R\bar{3}$ ($a^-a^-a^-$) above 1310 K. At the same time, the Mg/Ti ordering rate was found to remain unchanged (∼94%) over the whole temperature range investigated. The first-order phase transition from the monoclinic to the rhombohedral structure occurs without any intermediate phase. The discontinuous character of this structure transformation is also confirmed by the temperature variation of the in-phase tilt angle in the vicinity of the phase transition. Since the temperature coefficient of the dielectric permittivity changes sign at this type of structure transformation, the obtained data on the $P2_1/n$–$R\bar{3}$ crossover can be useful for development of the temperature-compensated materials derived from LMT-based perovskite solid solutions.

Specific variations of the Ti–O bond lengths and the TiO_6 octahedra volume are observed both at the discontinuous phase transition and in the temperature interval about 170–300 K where the crystal structure of LMT remains monoclinic $P2_1/n$. The variations of these parameters correlate with the dielectric anomalies in LMT revealed in the vicinity of room temperature. Deformations of the oxygen octahedra caused by some relaxation-like process in the crystal lattice are believed to affect the dielectric behaviour of LMT.

Acknowledgments

The first author acknowledges the Foundation for Science and Technology (FCT-Portugal, grant SFRH/BPD/14988/2004) for their financial support. The neutron diffraction experiment in BENSC has been supported by the European Commission under the 6th Framework Programme through the Key Action: Strengthening the European Research Infrastructures. Contract no RII3-CT-2003-505925 (NMI 3).

References

[1] Cava R J 2001 *J. Mater. Chem.* **11** 54
[2] Reaney I M, Colla E L and Setter N 1994 *Japan. J. Appl. Phys.* **33** 3984

[3] Colla E L, Reaney I M and Setter N 1993 *J. Appl. Phys.* **74** 3414
[4] Harrop P J 1960 *J. Mater. Sci.* **4** 370
[5] Seabra M P, Avdeev M, Ferreira V M, Pullar R C and Alford N McN 2003 *J. Eur. Ceram. Soc.* **23** 2403
[6] Seabra M P, Salak A N, Ferreira V M, Vieira L G and Ribeiro J L 2004 *J. Eur. Ceram. Soc.* **24** 2995
[7] Negas T, Yeager G, Bell S and Amren R 1991 *Chemistry of Electronic Ceramic Materials* (Lancaster PA: Technomic) pp 21–34
[8] Cho S Y, Kim C H, Kim D W, Hong K S and Kim J H 1999 *J. Mater. Res.* **14** 2484
[9] Salak A N, Seabra M P, Ferreira V M, Ribeiro J L and Vieira L G 2004 *J. Phys. D: Appl. Phys.* **37** 914
[10] Salak A N, Khalyavin D D, Senos A M R, Mantas P Q and Ferreira V M 2005 *J. Appl. Phys.* **98** 034101
[11] German M and Kovba L M 1983 *Russ. J. Inorg. Chem.* **28** 586
[12] Meden A and Ceh M 1998 *Mater. Sci. Forum* **773** 278
[13] Lee D Y, Yoon S J, Yeo J H, Nahm S, Paik J H, Whang K C and Ahn B G 2000 *J. Mater. Sci. Lett.* **19** 131
[14] Glazer A M 1972 *Acta Crystallogr.* B **28** 3384
[15] Avdeev M, Seabra M P and Ferreira V M 2002 *J. Mater. Res.* **15** 1112
[16] Vanderah T A, Miller V L, Levin I, Bell S M and Negas T 2004 *J. Solid State Chem.* **177** 2023
[17] Kipkoech E R, Azough F and Freer R 2005 *J. Am. Ceram. Soc.* **88** 768
[18] Seabra M P and Ferreira V M 2002 *Mater. Res. Bull.* **37** 255
[19] Rodriguez-Carvajal J 1993 *Physica* B **192** 55
[20] Hakki B W and Coleman P D 1960 *IRE Trans. Microw. Theory Tech.* **8** 402
[21] Kobayashi Y and Katoh M 1985 *IEEE Trans. Microw. Theory Tech.* **33** 586
[22] Levin I, Vanderah T A, Amos T G and Maslar J E 2005 *Chem. Mater.* **17** 3273
[23] Salak A N and Ferreira V M 2006 *J. Phys.: Condens. Matter* **18** 5703
[24] Howard C J, Kennedy B J and Woodward P M 2003 *Acta Crystallogr.* B **59** 463
[25] Gateshki M, Igartua J M and Hernandez-Bocanegra E 2003 *J. Phys.: Condens. Matter* **15** 6199
[26] Zhou Q, Kennedy B J, Howard C J, Elcombe M M and Studer A J 2005 *Chem. Mater.* **17** 5357
[27] Macquart R B and Kennedy B J 2005 *Chem. Mater.* **17** 1905
[28] Kennedy B J, Howard C J, Knight K S, Zhang Z and Zhou Q 2006 *Acta Crystallogr.* B **62** 537
[29] Hayward S A, Redfern S A T and Salje E K H 2002 *J. Phys.: Condens. Matter* **14** 10131
[30] Salje E K H 1990 *Phase Transitions in Ferroelastic and Co-elastic Crystals* (Cambridge: Cambridge University Press)
[31] Hayward S A, Morrison F D, Redfern S A T, Salje E K H, Scott J F, Knight K S, Tarantino S, Glazer A M, Shuvaeva V, Daniel P, Zhang M and Carpenter M A 2005 *Phys. Rev.* B **72** 054110
[32] Anderson M T, Greenwood K B, Taylor G A and Poeppelmeir K R 1993 *Prog. Solid State Chem.* **22** 197
[33] Woodward P M 1997 *Acta Crystallogr.* B **53** 443
[34] Levin I, Chan J Y, Maslar J E, Vanderah T A and Bell S M 2001 *J. Appl. Phys.* **90** 904
[35] Cheah M C L, Kennedy B J, Withers R L, Yonemura M and Kamiyama T 2006 *J. Solid State Chem.* **179** 2487
[36] Ubic R, Hu Y and Abrahams I 2006 *Acta Crystallogr.* B **62** 521
[37] Bhalla A S, Guo R and Roy R 2000 *Mater. Res. Innov.* **4** 3
[38] Zurmuhlen R, Petzelt J, Kamba S, Voitsekhovski V V, Colla E and Setter N 1995 *J. Appl. Phys.* **77** 5341
[39] Zurmuhlen R, Petzelt J, Kamba S, Kozlov G, Volkov A, Gorshunov B, Dube D, Tagantsev A and Setter N 1995 *J. Appl. Phys.* **77** 5351
[40] Goodenough J B 2004 *Rep. Prog. Phys.* **67** 1915
[41] Wise P L, Reaney I M, Lee W E, Iddles D M, Cannell D S and Price T J 2002 *J. Mater. Res.* **17** 2033
[42] Seabra M P, Salak A N, Avdeev M and Ferreira V M 2003 *J. Phys.: Condens. Matter* **15** 4229
[43] Groen W A, van Berkel F P F and Ijdo D J W 1986 *Acta Crystallogr.* C **42** 1472
[44] Wersing W 1991 *Electronic Ceramics* (London: Elsevier) pp 67–119